Direct Position Determination for TDOA-based Single Sensor Localization

CHRISTIAN STEFFES
MARC OISPUU

In this paper, four different localization techniques based on TDOA-measurements for single sensor passive emitter localization are proposed. The use of signal structure information allows TDOA-based localization with a single moving sensor node. A direct position estimation scheme is derived for the single sensor TDOA localization problem. The feasibility of the proposed method is shown in simulations. The position estimation accuracy of the single sensor TDOA and the direct technique are compared using simulation results and the Cramér-Rao Lower Bound. Field experiments using an airborne sensor are conducted to prove the concept.

Manuscript received October 30, 2015; revised March 4, 2016; released for publication June 13, 2016.

Refereeing of this contribution was handled by Gerhard Kurz.

Authors' address: Dept. Sensor Data and Information Fusion, Fraunhofer Institute for Communication, Information Processing and Ergonomics FKIE, Fraunhoferstr. 20, 53343 Wachtberg, Germany. (E-mail: {christian.steffes, marc.oispuu}@fkie.fraunhofer.de).

1557-6418/16/$17.00 © 2016 JAIF

I. INTRODUCTION

Passive emitter localization is a fundamental task encountered in various fields like wireless communication, radar, sonar, seismology, and radio astronomy. An airborne sensor platform is the preferable solution in many applications. The sensor is typically mounted e.g. on an aircraft, a helicopter, or an unmanned aerial vehicle (UAV). Airborne sensors provide in comparison to ground located sensors a far-ranging signal acquisition because of the extended radio horizon. Mostly for localization issues, sensors are installed under the fuselage or in the wings of the airborne sensor platform. In case of hard payload restrictions only compact sensors come into consideration.

Aspects of the two-dimensional and three-dimensional localization problem examined in the literature include numerous estimation algorithms, estimation accuracy, and target observability [16], [3]. Typical localization systems of interest obtain measurements like direction of arrival (DOA), frequency difference of arrival (FDOA), time difference of arrival (TDOA) or combinations of the aforementioned measurements [6].

Commonly, the desired source locations are determined in multiple steps: the signal processing step where the sensor data is computed from the raw signal data, and the sensor data fusion step where the localization and tracking task is performed. Alternatively, direct position determination (DPD) approaches have been proposed to compute the desired target parameters in a single step based on the raw signal data without explicitly computing intermediate measurements like DOA, FDOA, and TDOA [19], [18]. It has been shown that this kind of data processing offers a superior performance in scenarios with weak or closely-spaced sources but requires a higher computational burden in comparison to the standard multi-step processing. For example for TDOA-based localization, a direct approach based on the raw signal data has been proposed in [19], [1], and a standard approach based on TDOA/FDOA measurements has been proposed in [15], [16], respectively. In [10], a localization approach based on the complex ambiguity function (CAF) has been introduced which turned out to be a compromise between localization performance and computational burden. Analysis of emitter localization using a single moving observer based on frequency measurements with context knowledge has been introduced in [4]. The results show the advantage of using a priori knowledge concerning the emitter's altitude (either known or using a terrain model) on the performance of a localization system. In [2], a method for single platform geolocation using joint Doppler and AOA measurements is proposed. The combination of these heterogeneous measurements can allow more accurate position estimation. More recently, research on the single receiver TOA/TDOA-based localization using the periodicity of emitted signals has attracted attention. In [17], the single observer geolocation dealing

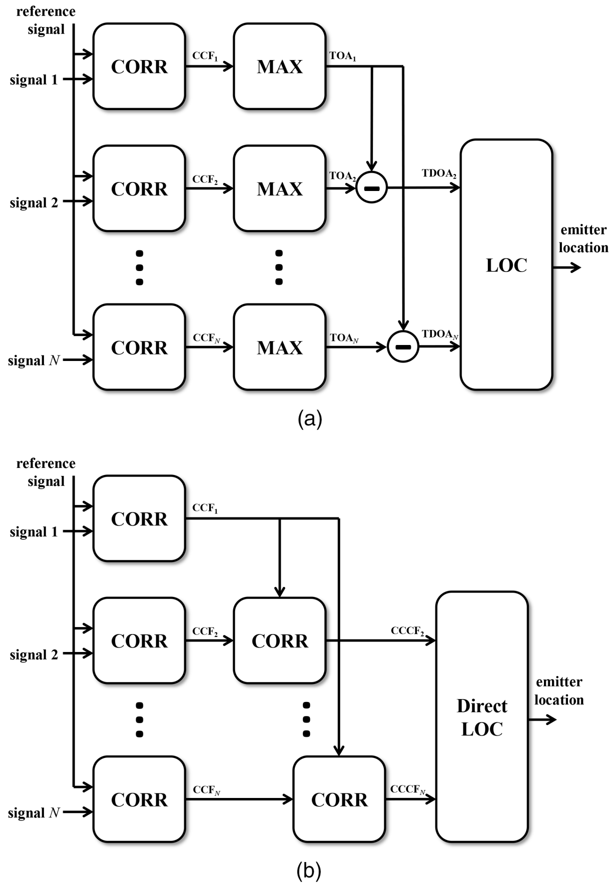

Fig. 1. Comparison of non-direct and direct S^{4}TDOA approach. (a) S^{4}TDOA approach. (b) DS^{4}TDOA.

with oscillator instability is investigated. Experimental results using a moving observer and Kalman filters for the estimation of the local oscillator drift can be found in [7], [11].

In our previous work, we proposed a DPD approach for a moving antenna array sensor [9], [8]. Furthermore in [13], we introduced a *single element* TDOA localization approach using just a single omni-directional antenna. In the following, this approach is referred to as single sensor signal structure TDOA (S^{4}TDOA) localization (Fig. 1(a)). Commonly, single-element approaches using a single directional antenna take the directions in which local maximum power is received to be the DOA estimates [12]. Since directional antennas cannot simultaneously scan in all directions, some transient signals can escape detection and fluctuations of the source signal strength and polarization during the sequential lobing process may have a significant impact on the DOA accuracy. However, these problems are circumvented by the technique proposed in [13] which is applicable when information about the signal structure is a priori known (e.g. communication and radar emitters). The method does not require knowledge of the contents of the emitted signal. The information that is needed, is that the emitter sends message bursts at a known repetition frequency. For the example of GSM signals, the emitter sends data of a duration of ≈ 546.46 μs followed by a pause of ≈ 30.46 μs. The knowledge of this repeated pattern of signal transmissions and pauses is used for the single sensor signal structure TDOA approach. In this paper, we assume the transmission on/off structure to be known but never assume the transmitted signal itself to be known to the estimator during the simulations and real data evaluation.

In [14], the single-element TDOA localization approach is extended by the key-idea of direct emitter localization. For an airborne scenario with a single stationary source, we introduce a novel direct localization approach based on the cross correlation function (CCF). Our simulation and experimental measurement results demonstrate that the proposed approach considerably outperforms the standard single-element localization approach. This approach is named as direct S^{4}TDOA abbreviated with DS^{4}TDOA (Fig. 1(b)).

The block diagram given in Fig. 1 depicts the different approaches in the measurement/localization steps. For the non-direct S^{4}TDOA method, the signal received at each observation step is correlated with the reference signal. The maximum of this correlation yields the TOA of the signal. By differentiating TOAs of two observation steps, a TDOA measurement is obtained (first step: measurement step). These TDOA measurements are used in the localization step (2nd step). The direct method DS^{4}TDOA omits the TDOA estimation step and the correlation functions are input to the localization algorithm (Direct Position Determination, single step localization).

This paper is based on the work presented in [14]. Two slightly different (D)S^{4}TDOA are described. The newly introduced methods are called (D)S^{4}TDOA* and do not rely on the explicit representation of the signal structure using a reference signal. All four (D)S^{4}TDOA$^{(*)}$ approaches are compared using the Cramér-Rao Lower Bound CRLB and Monte-Carlo simulations.

This paper is organized as follows: In Section II, the considered localization problem is stated. The Cramér-Rao Lower Bounds on TDOA estimation and on TDOA-based emitter localization are described in Section III. In Section IV, we briefly review the S^{4}TDOA localization approach based on the CAF [13] as well as the direct version DS^{4}TDOA [14] and introduce the two novel (D)S^{4}TDOA* approaches. Monte-Carlo simulations and the comparison to the Cramér-Rao Lower Bound are shown in Section V. Simulation results for a real data scenario comparing S^{4}TDOA and DS^{4}TDOA approaches are presented in Section VI. In Section VII, the experimental measurement results proof the concept. Finally, the conclusions are given in Section VIII.

The following notations are used throughout this paper: $f[k]$ is a discrete version of the function $f(t)$, $f^*[k]$ is the conjugate complex of the function $f[k]$,

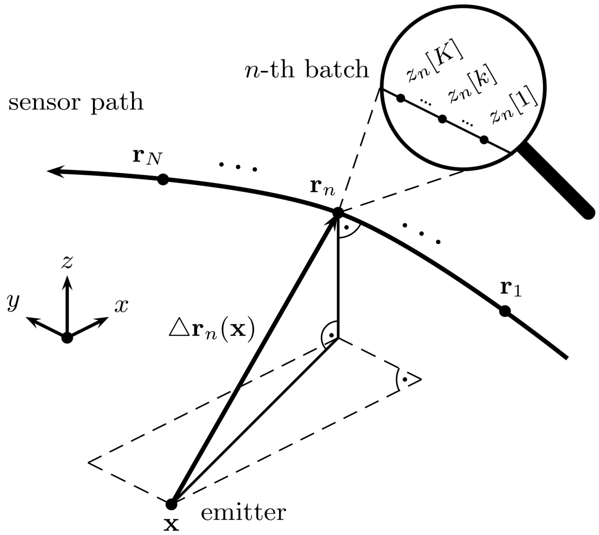

Fig. 2. Three-dimensional localization scenario.

$f^{(\tau)}[k]$ denotes the sampled version of $f(t-\tau)$ and $(\cdot)^T$ denotes transpose.

II. PROBLEM FORMULATION

We consider an omni-directional antenna sensor mounted on an airborne platform moving along an arbitrary but known sensor path observing a single stationary, ground-located source at position $\mathbf{x}$. The target emits a coherent signal $s(t)$ which is built up by times, where information is transmitted and pause intervals between those transmissions. The duration of each transmissions and each pause intervals is assumed to be constant and known. For example in the case of a communication signals, the information is sent as bursts during the transmission time and the pause times are guard periods between consecutive bursts. The exact modulation method or the content of the transmission bursts doesn't need to be known as long as a certain level of signal-to-noise ratio results from the transmission.

During the movement, the sensor collects N signal data batches. The nth received signal at some measurement point reads

$$z_n(t) = a_n s(t - t_{e,n} - t_n)\exp(\mathrm{j}\nu_n t) + w_n(t), \tag{1}$$

where a_n denotes a path attenuation factor, $t_{e,n}$ denotes the unknown signal emission time of the nth received signal, t_n denotes the time difference between signal emission and signal acquisition, ν_n is the signal Doppler shift induced by the movement of the own sensor platform, and w_n denotes some additional receiver noise, $n = 1,\ldots,N$. The transmitted signal $s(t)$ and the received signals $z_n(t)$ are assumed to be complex base-band signals.

In practice, the sensor collects data samples from the received signal. In the considered scenario, the sampling rate is assumed to be high enough that the sensor location $\mathbf{r}_n$ is approximately constant for each collected data batch (Fig. 2). Then, t_n and ν_n are given by

$$t_n(\mathbf{x}) = \frac{\|\triangle\mathbf{r}_n(\mathbf{x})\|}{c}, \tag{2}$$

$$\nu_n(\mathbf{x}) = \frac{\mathbf{v}_n^T \triangle\mathbf{r}_n(\mathbf{x})}{\|\triangle\mathbf{r}_n(\mathbf{x})\|}\frac{f_0}{c}, \tag{3}$$

respectively, where $\triangle\mathbf{r}_n(\mathbf{x}) = \mathbf{x} - \mathbf{r}_n$ denotes the relative vector between sensor and source, $\mathbf{v}_n$ is the sensor velocity vector, c is the signal propagation speed, and f_0 is the center frequency of the emitted signal.

Considering the time-discrete version of the received signal in (1), the kth data sample of the nth data batch is given by

$$z_n[k] = a_n s(k\triangle - \mathrm{clk}_n - \tau_n)\exp(\mathrm{j}\nu_n k\triangle) + w_n[k], \tag{4}$$

where $\triangle$ is the sample interval, clk_n is the known sensor clock of the nth measurement, τ_n is the signal time of arrival relative to the sensor clock. Please note that $\mathrm{clk}_n + \tau_n = t_{e,n} + t_n$ holds. The additional receiver noise w_n is assumed to be temporally uncorrelated and zero-mean Gaussian.

For the single sensor TDOA estimation, a reference signal $\tilde{s}[k]$ is used which characterizes the repetition pattern of the transmitted signal. For the ideal case, the emitted signal would be known and thus $\tilde{s}[k] = s[k]$. Since usually, the emitted signal is unknown for almost all applications, the reference signal we employ throughout this paper only characterizes the transmission on/off pattern of the emitted signal, which basically results in a comparison of the amplitudes of the received signal with the reference signal. If the emitted signal were known, much better localization performance could be achieved. Throughout this paper, we assume the transmission and guard interval periods to be known. The method doesn't require knowledge of the contents of the emitted signal and we never assume the signal to be known during the simulations or real data evaluation (where in fact, we don't know the emitted signal).

Finally, the localization problem is stated as follows: Estimate the source location $\mathbf{x}$ from the received signal data batches $\mathbf{z}_n = (z_n[1],\ldots,z_n[K])^T$, $n = 1,\ldots,N$.

III. CRAMÉR-RAO LOWER BOUND

The CRLB provides a lower bound on the estimation accuracy and its parameter dependencies reveal characteristic features of the estimation problem. The parameters to be estimated from the measurements $\mathbf{z} = (\mathbf{z}_1^T,\ldots,\mathbf{z}_N^T)^T$ are given by the vector $\mathbf{x}$. In this case, the CRLB is related to the covariance matrix $\mathbf{C}$ of the estimation error $\triangle\mathbf{x} = \mathbf{x} - \hat{\mathbf{x}}(\mathbf{z})$ of any unbiased estimator $\hat{\mathbf{x}}(\mathbf{z})$ as

$$\mathbf{C} = \mathrm{E}\{\triangle\mathbf{x}\triangle\mathbf{x}^T\} \geq \mathbf{J}^{-1}(\mathbf{x}), \tag{5}$$

where the inequality means that the matrix difference is positive semidefinite and $\mathbf{J}$ is the Fisher Information

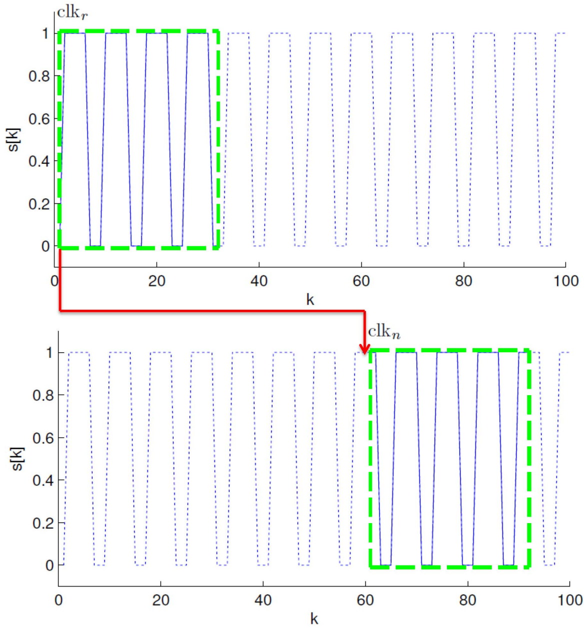

Fig. 3. Schematic representation of the received signals at measurement step r and n.

Matrix (FIM) given by

$$\mathbf{J}(\mathbf{x}) = \mathrm{E}\left\{ \left(\frac{\partial \mathcal{L}(\mathbf{z};\mathbf{x})}{\partial \mathbf{x}} \right) \left(\frac{\partial \mathcal{L}(\mathbf{z};\mathbf{x})}{\partial \mathbf{x}} \right)^T \right\}, \tag{6}$$

where $\mathcal{L}$ denotes the log-likelihood function. If the estimator attains the CRLB then it is called *efficient*. The CRLB is given by the inverse Fisher Information.

In the following sections, CRLB for the TDOA estimation (Section III-A) as well as for the localization problem (Section III-B) are described.

A. CRLB on TDOA Estimation

The problem of estimating the TDOA τ of received signals can be stated as follows. From a set of signals $z_n(t)$, estimate the corresponding TDOAs. A lower bound on the achievable accuracy of this estimation process is essential for the calculation of the achievable localization accuracy described in Section III-B.

One of the most cited publication in this field is the work of Stein [15]. A CRLB on TDOA/FDOA estimation for the acoustic case is derived based on signal parameters like the bandwidth, the integration time and the signal-to-noise ratio of the received signals. The signals are assumed to be stationary Gaussian random processes. A more clear distinction between acoustic and electromagnetic signals was for example introduced in [5]. A more generalized bound for deterministic unknown signals was presented in [20]. The bound is determined using a given realization of the emitted signal itself. We use the Fisher Information $\mathbf{J}_\tau$ for the CRLB on emitter localization in the following section.

B. CRLB on Emitter Localization

The Fisher information for the TDOA-based localization problem is

$$\mathbf{J}(\mathbf{x}) = \sum_m \left(\left(\frac{\partial \tau_m}{\partial \mathbf{x}} \right) \mathbf{J}_\tau \left(\frac{\partial \tau_m}{\partial \mathbf{x}} \right)^T \right), \tag{7}$$

where m gives the TDOA measurement index and $\sigma^2_{\tau_m}$ is the variance of the corresponding TDOA estimation process modeled by the CRLB found in [20].

The CRLB for the position estimation accuracy is then given by

$$\sigma^2_{\mathbf{x}} = \mathrm{tr}(\mathbf{J}^{-1}(\mathbf{x})). \tag{8}$$

If TDOA measurements are temporally and spatially uncorrelated, the addition of the Fisher information of different measurement steps is possible.

IV. LOCALIZATION APPROACHES

In this section, approaches for the stated localization problem are presented i.e. the localization of a source with periodic coherent emission using a single moving sensor. Four measurement approaches for the single observer scenario are considered.

Firstly, an approach S^{4}TDOA based on TOA measurements is presented (Section IV-A). Then, a derivation of this method called DS^{4}TDOA based on the CCF and direct position determination is presented in Section IV-B. For both methods, approaches without the use of a representation of the reference signal $\tilde{s}[k]$ are introduced in Section IV-D. Those methods are called S^{4}TDOA* and DS^{4}TDOA* respectively. For the sake of simplicity, only TOA/TDOA measurements are considered in following and the Doppler is neglected. Nevertheless, the following techniques could be generalized to full CAF.

A. Two-step S^{4}TDOA Approach [13]

Step 1: Commonly for a sensor network, TDOA measurements are extracted from the CCF

$$\mathrm{CCF}(\triangle\tau) = \sum_{k=1}^{K} z_1^*[k] z_2^{(-\triangle\tau)}[k], \tag{9}$$

i.e. from the correlation of the two signals $z_1[k]$ and $z_2[k]$ in time domain. The TDOA estimates are calculated by detecting the peak in the CAF:

$$\triangle\hat{\tau} = \arg\max_{\triangle\tau} \mathrm{CCF}(\triangle\tau). \tag{10}$$

However, since a single moving sensor is considered, the measurements are not taken simultaneously. Thus in the following, the signal processing for the single sensor case is presented (Fig. 1(a)). Due to the known signal structure, a quasi-TDOA measurement can be computed by considering the individual known sensor clock clk$_n$:

$$\hat{\tau}_n = \arg\max_{\tau} \mathrm{CCF}_n(\tau) \tag{11}$$

with

$$\mathrm{CCF}_n(\tau) = \sum_{k=1}^{K} z_n^*[k]\tilde{s}^{(-\mathrm{clk}_n-\tau)}[k], \tag{12}$$

where $\tilde{s}[k]$ denotes a reference signal introduced in (4). Then similar to (10), a quasi-TDOA measurement can be calculated by taking the clock differences (Fig. 3)

$$\triangle\mathrm{clk}_{n,r} = \left(\left\lceil \frac{\mathrm{clk}_n - \mathrm{clk}_r}{T} \right\rceil - \left\lfloor \frac{\mathrm{clk}_n - \mathrm{clk}_r}{T} \right\rfloor \right) T \tag{13}$$

into account, where the index r indicates some reference time. Then a quasi-TDOA measurement can be extracted from the TOA estimates by

$$\triangle\hat{\tau}_{n,r} = \hat{\tau}_n - (\hat{\tau}_r + \triangle\mathrm{clk}_{n,r}), \tag{14}$$

i.e. by the difference of the individual estimated TOAs corrected by the clock difference. The correction of the clock difference is mandatory because the measurements are not taken simultaneously.

Step 2: The emitter localization problem can be solved by searching the emitter location that most likely explains the TDOA measurements calculated in (14). Therefore, the emitter location can be calculated by solving the following least-squares form:

$$\hat{\mathbf{x}} = \arg\min_{\mathbf{x}} \sum_{\substack{n=1\\ n\neq r}}^{N} \frac{\| \triangle\hat{\tau}_{n,r} - \triangle\tau_{n,r}(\mathbf{x})\|^2}{\sigma^2_{\triangle\tau,n,r}}, \tag{15}$$

where $\triangle\tau_{n,r}(\mathbf{x})$ denotes the measurement function given analog to (14) by

$$\triangle\tau_{n,r}(\mathbf{x}) = t_n(\mathbf{x}) - (t_r(\mathbf{x}) + \triangle\mathrm{clk}_{n,r}), \tag{16}$$

according to (2) and $\sigma^2_{\triangle\tau,n,r}$ denote the TDOA measurement variance, $n = 1,\ldots,N$. The solution in (15) can be geometrically interpreted as the intersection of the hyperbolae represented by the individual TDOA measurements.

At this point it is worth to mention that in practice, the measurement variances are unknown and vary during the time. Consequently, the measurement variance have to be estimated because otherwise one could use an estimator with a reduced performance.

B. One-step DS^{4}TDOA Approach [14]

The key-idea of direct localization approaches is to avoid the decision for one TOA/TDOA/AOA measurement in the first step of a localization algorithm. In the case of the S^{4}TDOA method as described in the previous section, this decision is represented by the process of maximum determination of the CCF. The choice will always falls on the highest peak of the CCF, but when taking into account all measurement batches, this peak might be wrong. In this case, f.e. the second highest peak of the CCF would correspond to the sensor emitter geometry and fit all other measurement batches. Thus, leaving this decision open, allows the implicit evaluation of multiple measurement hypotheses in one localization step.

The intention is to create a cost function that has to be optimized in the localization step, which takes into account all measurement batches at the same time without the explicit decision for TDOAs (Fig. 1(b)). By calculating the CCF of the CCF_r (CCF of $\mathbf{z}_r$ and $s[k]$) and the CCF_n (CCF of $\mathbf{z}_n$ and $s[k]$), the choice for an explicit TDOA can be postponed into the localization step. We call this approach direct single-sensor signal structure TDOA localization (DS^{4}TDOA).

The choice of this approach is motivated by the scheme used for the multi-sensor TDOA localization, where the TDOA is not explicitly chosen in the first step but the TDOA measurement function is directly used as input for the localization step [1], [10]. Instead of a TDOA estimation from two received signals, DS^{4}TDOA obtains the TDOA from two TOA measurements. The equivalent DS^{4}TDOA then relies on the CCF of the TOA measurement functions, which are the CCFs of the received signals with the reference signal.

The proposed cost function (cross correlation of cross correlation functions) subject to the position $\mathbf{x}$ is defined as

$$\mathrm{CCCF}_{n,r}(\mathbf{x}) = \sum_{k=1}^{K} \mathrm{CCF}_n^*[k]\mathrm{CCF}_r^{(-\triangle\tau_n(\mathbf{x}))}[k], \tag{17}$$

with the CCF given in (12). The localization problem is then stated by

$$\hat{\mathbf{x}} = \arg\max_{\mathbf{x}} \sum_{\substack{n=1\\ n\neq r}}^{N} \mathrm{CCCF}_{n,r}(\mathbf{x}). \tag{18}$$

C. Discussion

The localization accuracy for both methods may degrade, if the distance between two observer positions is too big compared to the signal repetition duration T. If $\triangle\tau_n(\mathbf{x}) \geq T/2$ the wrong peak may be chosen in the maximum determination of the CCFs in the case of S^{4}TDOA. This choice has a direct effect on the localization accuracy using S^{4}TDOA.

The influence on the localization for DS^{4}TDOA is smaller if $\triangle\tau_n(\mathbf{x}) < T/2$ for almost all n. If $\triangle\tau_n(\mathbf{x}) \geq T/2$ for a significant number of measurements, the optimization of the localization function (18) may run into the maximum that corresponds to the wrong time slots. However this is unlikely, because the ambiguities that are due to $\triangle\tau_n(\mathbf{x}) \geq T/2$ are unlike to join in the same spatial position unless more than one emitter is present.

D. (D)S^{4}TDOA without the use of $\tilde{s}[k]$

Both approaches described in the previous sections use an additional signal $\tilde{s}[k]$ representing the information on the signal structure. This allows data reduction for the localization step. If processing power and data storage capacity and—in case of the use of the methods with multiple sensors—communication bandwidth is not an issue, the received signals can be stored and used for the localization process. In this case, instead of using TOA estimates calculated using $\tilde{s}[k]$ for S^{4}TDOA and the CCCF for DS^{4}TDOA, the cross correlation function of two received signals is used to estimate the TDOA or in the cost function of the direct method respectively. An additional shift factor according to the signal repetition interval and the observation time span has to be taken into account. We call these methods S^{4}TDOA* and DS^{4}TDOA*.

S^{4}TDOA*:

The first step of the localization process of S^{4}TDOA* is to calculate the maximum of the cross correlation function of two received signals at different time steps n, r:

$$\mathrm{CCF}_{n,r}(\tau) = \sum_{k=1}^{K} z_n^*[k] z_r^{(-\mathrm{clk}_{n,r}-\tau)}[k]. \tag{19}$$

The TDOA measurement is then given by

$$\hat{\tau}_{n,r} = \arg\max_{\tau} \mathrm{CCF}_{n,r}(\tau). \tag{20}$$

In the second step, the emitter position is estimated by solving (15).

DS^{4}TDOA*:

Similar to (17), the cost function for DS^{4}TDOA* is given by

$$\mathrm{CCF}_{n,r}(\mathbf{x}) = \sum_{k=1}^{K} z_n^*[k] z_r^{(-\triangle\tau_n(\mathbf{x}))}[k]. \tag{21}$$

The localization problem is then stated by

$$\hat{\mathbf{x}} = \arg\max_{\mathbf{x}} \sum_{\substack{n=1 \\ n\neq r}}^{N} \mathrm{CCF}_{n,r}(\mathbf{x}). \tag{22}$$

For the evaluation of the real measurement data in this paper (sections VI and VII), S^{4}TDOA* and DS^{4}TDOA* are not applicable since processing power and storage capacity were limited. In the theoretical simulation and the CRLB evaluation (see section V), all four (D)S^{4}TDOA$^{(*)}$ methods are compared.

V. LOCALIZATION ACCURACY EVALUATION

A. Simulation Setup

To evaluate the four presented (D)S^{4}TDOA$^{(*)}$ localization approaches, Monte-Carlo simulations and CRLB analysis are conducted. A 2-dimensional scenario is investigated where one observer moves along a trajectory from west to east as depicted in Fig. 4. For each observation time step $n = 1 \ldots 12$, a signal $s_n[k]$ that is emitted from the target is simulated. We assume free space path loss

$$\mathrm{FSPL}_{\mathrm{dB}} = 10\log_{10}\left(\frac{4\pi \| \triangle \mathbf{r}_n(\mathbf{x}) \|}{\lambda}\right)^2 \tag{23}$$

and, by taking the receiver sensitivity $\mathrm{S_{dB}}$ into account, calculate the corresponding SNR

$$\mathrm{SNR_{dB(n)}} = (\mathrm{P_E} + \mathrm{G_E} + \mathrm{G_R} - \mathrm{FSPL_{dB}}) - \mathrm{S_{dB}}, \tag{24}$$

where λ is the wavelength of the signal, $\mathrm{P_E}$ is the transmitter power, $\mathrm{G_E}$ and $\mathrm{G_R}$ are antenna gain of the emitter and receiver antennas. The received signal is delayed by the time $t_n(\mathbf{x})$ the signal took to travel from the emitter to the observer according to (2).

The signals for each observation step are simulated as complex valued base-band signals at a sample rate of $f_s = 400$ kHz using the following parameters. The duration of each observed signal is T = 1 ms composed of repeated data transmission $\mathrm{T_{data}} = 50\ \mu$s and guard periods with duration $\mathrm{T_{guard}} = 10\ \mu$s. During the time of data transmission, the emitted signal consists of a chirp signal with bandwidth B = 200 kHz. During the guard periods, no data is transmitted. White Gaussian noise is then added to the signal according to the SNR calculated using (24). The noise power is determined over the whole observation bandwidth of 400 Khz. The parameters for the path loss calculation are $\mathrm{G_E} = 3$ dB, $\mathrm{G_R} = 0$ dB, $\mathrm{S_{dB}} = -90$ dBm at a center frequency of 1800 MHz. The transmission power $\mathrm{P_E}$ is varied for different evaluations. The received signal is then given by $z_n[k]$.

The reference signal $\tilde{s}[k]$ which is used by (D)S^{4}TDOA has the same duration as the simulated received signal. The data transmission period starts with the first sample of $\tilde{s}[k]$ and the same reference signal is used at each time step. Since the TDOA and position estimation using (D)S^{4}TDOA in this special realization rely on the amplitude comparison by correlating the received signals z_n with the reference signal $\tilde{s}$, the reference signal can be modeled as a real valued signal with $\tilde{s}[k] = 1$ during data transmission periods and $\tilde{s}[k] = 0$ during guard periods.

TDOA measurements are taken between consecutive observation steps resulting in a total of $N/2$ TDOA measurements. The measurement set for each measurement index $m = 1, \ldots, N/2$ is given by $\{\hat{\tau}_{1,2}, \ldots, \hat{\tau}_{2m-1,2m}\}$.

The cost functions of (D)S^{4}TDOA$^{(*)}$ are maximized using Nelder Mead simplex optimization under the assumption of constant TDOA measurement variance. The initial position estimate for the optimization process is calculated by evaluating the cost functions on a grid of possible emitter positions. The grid points are spaced by 500×500 m. For the first TDOA measurement, no position estimate is given, since the emitter location is not observable with only one TDOA measurement.

Simulations with 500 Monte-Carlo runs are conducted. For each run, the emitter position is chosen uniformly at random from an area of interest ($\mathrm{AOI_x}$ =

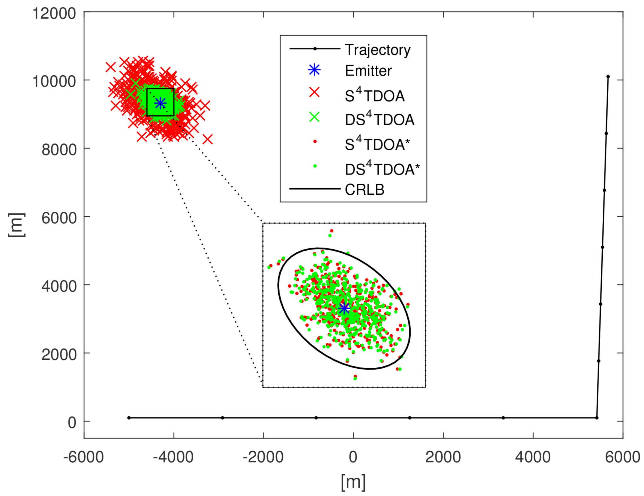

Fig. 4. Scenario used for localization accuracy analysis including results of (D)S^{4}TDOA. Zoom of target area shows only (D)S^{4}TDOA* results. Transmission power $P_E = 30$ dBm. CRLB is depicted as 3σ ellipse.

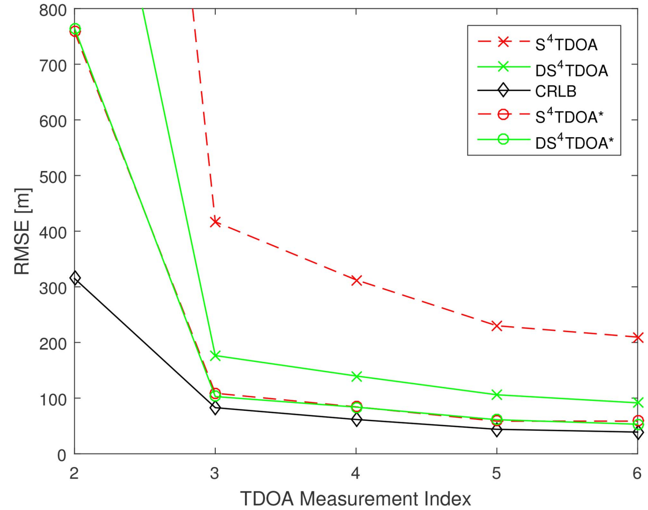

Fig. 6. Comparison of localization approaches to CRLB (transmission power $P_E = 30$ dBm).

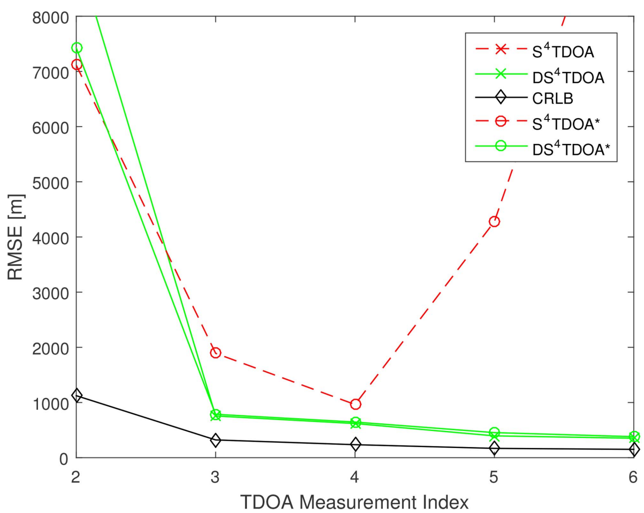

Fig. 5. Comparison of localization approaches to CRLB (transmission power $P_E = 18$ dBm).

$-5000,\ldots,5000$ m, $AOI_y = 1000,\ldots,8000$ m). The position is estimated using all four (D)S^{4}TDOA$^{(*)}$ methods and the corresponding localization CRLB is calculated according to (8).

B. Results

The simulations are carried out for different transmission powers. Fig. 5 shows the results for $P_E =$ 18 dBm. For many emitter positions throughout the area of interest, this results in low SNR values. Both direct localization approaches are more robust against low SNR, since ambiguities in the cross correlation functions have less effect on the localization. The two step localization methods need to chose one TDOA measurement in the first step independently of all other observation steps whereas the direct technique postpones this decision into the localization step, where all measurements are incorporated (see also Section IV-C). The similar accuracy of DS^{4}TDOA and DS^{4}TDOA* is due to the high repetition rate of transmission and guard periods. The correlation of the reference signal, having very high SNR, and the received signal with low SNR, still shows good cross correlation characteristics. The position estimation accuracy of S^{4}TDOA is out of the scale of Fig. 5. The performance of S^{4}TDOA* improves until measurement index 4 and then degrades again. This is due to the fact that the mean SNR for the given trajectory and randomized emitter positions from the area of interest is often lower at the last observation points and thus the probability of choosing a wrong peak of the CCF increases.

By increasing the signal transmission power to $P_E =$ 30 dBm and thus having higher SNR, the performance of S^{4}TDOA* is very similar to DS^{4}TDOA* for all measurement steps. The results are depicted in Fig. 6. Again, DS^{4}TDOA outperforms S^{4}TDOA, which shows the lowest localization accuracy.

To show the distribution of the position estimates of all four (D)S^{4}TDOA$^{(*)}$ methods, a fixed emitter position is chosen. For this scenario, again 500 Monte-Carlo runs are conducted. The results of TDOA measurement index 6 are depicted in Fig. 4. The zoomed area shows only the estimates of S^{4}TDOA* and DS^{4}TDOA*. The CRLB is given by a 3σ error ellipse.

The advantages of (D)S^{4}TDOA compared to (D)S^{4}TDOA* are given by less need for storage space and a reduction of processing power (and communication requirements). A trade-off between localization accuracy and sensor requirements is possible using (D)S^{4}TDOA.

VI. SIMULATION USING REAL DATA SCENARIO

The proposed localization approaches performances are evaluated in Monte-Carlo simulations for a given

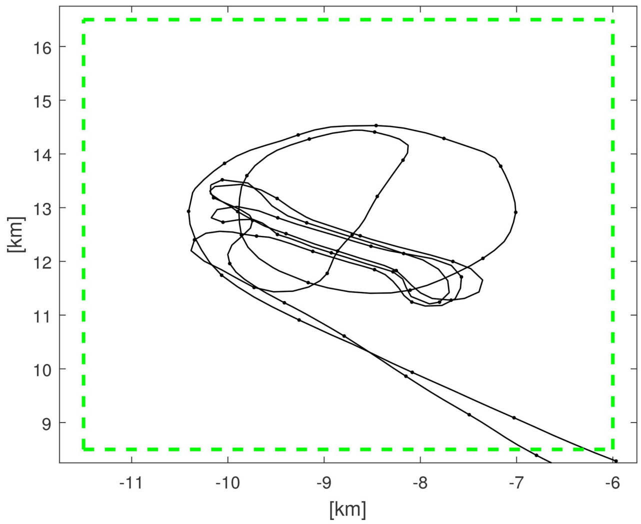

Fig. 7. Simulation Scenario: Sensor trajectory and area of interest (green box).

scenario. GSM base stations are chosen as emitter with recurring signal structure. In this section, only S^{4}TDOA and DS^{4}TDOA algorithms are evaluated.

A. Simulation Setup

The desired signal is sent on the broadcast channel of a GSM base station and is divided into time slots. Each time slot has a duration of 576.92 μs. A time slot is divided into data transmission time and guard period during which no transmission takes place. This time slot signal structure is represented by the reference signal $\tilde{s}[k]$ introduced in (4).

The sensor trajectory remains the same over all Monte-Carlo runs. The position of the emitter is chosen uniformly at random from a given area of interest. The localization accuracy is also evaluated w.r.t. the signal-to-noise ratio (SNR). A sensor trajectory that is similar to the one of the field experiments (Section VII) is used for the simulations. Fig. 7 shows the trajectory as well as the area of interest in which possible emitters are located.

We use the following definition of SNR for the simulations:

$$\mathrm{SNR}_{[\mathrm{dB}]} = 10\log_{10}\frac{P_s}{P_n} \tag{25}$$

with $\mathrm{P_s}$ being the mean signal power and $\mathrm{P_n}$ the mean noise power. A total of 250 Monte-Carlo runs were performed. Each Monte-Carlo run consists of the following:

1) An emitter position is chosen at random from the area of interest.
2) A random start drift of the broadcast signal is generated.
3) Signal noise for each sensor is generated.
4) For the given observer trajectory and emitter position and time of measurement, corresponding TOAs are calculated.
5) The broadcast signal is embedded into noise in accordance to the respective TOAs and scaled to meet given SNR value.
6) Localization results are calculated using both estimation methods
   a) The initialization is done by evaluating a grid of the respective cost functions for the area of interest.
   b) The position is estimated using Nelder Mead simplex optimization.
7) Points 5 to 6 are repeated for all SNR values in question.

B. Position Estimation

The position estimation for the S^{4}TDOA method is divided into two main steps. In the first step, the received signal is correlated with the stored reference signal. The maximum of this correlation function yields the TOA of each measurement. TOAs of two observation steps form one TDOA measurement. In the second step, the emitter position is estimated based on a set of TDOA measurements.

For the DS^{4}TDOA localization, from the two observation steps that form the TDOA measurement in the above described case, cross correlate the cross correlation functions of the respective received signals and the reference signal. Estimate the emitter position from a set of those cross correlation functions.

For both methods, the respective cost functions are minimized using Nelder/Mead simplex optimization. The initialization problem is solved by evaluating the cost functions of each method for a grid over the area of interest. For the simulations, the grid points were spaced by 100×100 m.

C. Results

Fig. 8 depicts the results of the simulations. For each SNR value, the RMSE of the position estimation over all 250 simulation runs is calculated. The red line with red dots shows the RMSE using the S^{4}TDOA, DS^{4}TDOA is plotted using red diamonds. The accuracy of the DS^{4}TDOA localization approach outperforms the S^{4}TDOA localization method.

VII. EXPERIMENTAL RESULTS

A. Experimental Setup

Field experiments were conducted to verify the presented method for real data. A GPS time-synchronized sensor node was used to gather data from a GSM mobile station. The sensors receiving antenna was mounted under the wing of an aircraft. The sensor itself and a PC for data processing were installed inside the aircraft.

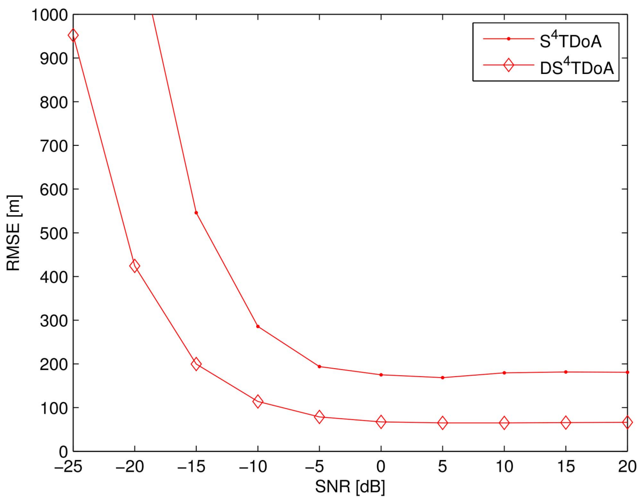

Fig. 8. Simulation results: Localization RMSE over SNR for DS⁴TDOA (red diamonds) and S⁴TDOA (red dots).

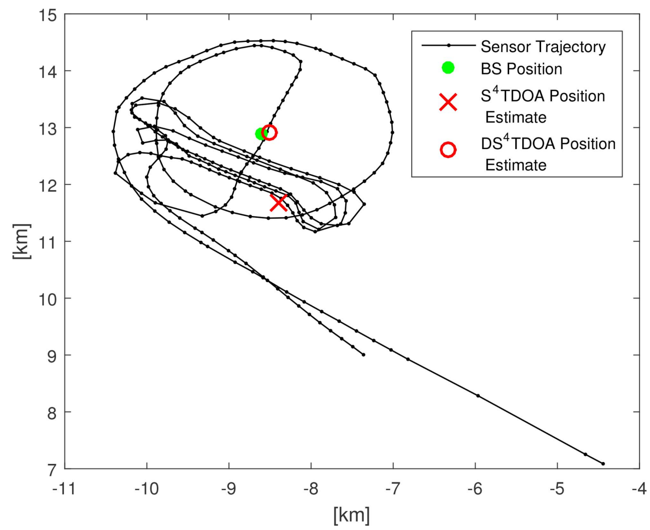

Fig. 9. Scenario of field experiments. Sensor trajectory and localization results.

Every five seconds, data from the broadcast channel of the GSM base station was recorded at a sample rate of $f_s = 1$ MHz.

Along with the signal data, corresponding timestamps and position information from the GPS receiver of the sensor are recorded. For each observation time step n, the received signals are filtered and the CCF is calculated. From this CCF the TOA $\hat{\tau}_n$ of the signal is estimated as described in Section IV. The CCF, the estimated TOA, the sensors position and time are used in the localization step. The localization estimates for both methods are calculated using the same initialization for the optimization algorithm.

Fig. 9 depicts the sensors trajectory, the position of the GSM base station as well as the localization results using the presented S⁴TDOA and DS⁴TDOA method. The presented localization approach is evaluated for different levels of signal strength. Here, a threshold P_t is applied to the measurements. If the mean received signal strength $P_{z_n[k]}$ is below the threshold, the measurement is not used in the localization step. The mean signal strength of a signal $z_n[k]$ is defined as

$$P_{z_n[k]} = \frac{z_n^*[k] z_n[k]}{K} \tag{26}$$

with K being the total number of samples.

B. Results

Fig. 10 to Fig. 13 show the localization cost functions evaluated for a grid of possible emitter positions. The black line indicates the flight trajectory where the black dots indicate the measurements that are taken into account in the localization step according to the received signal strength threshold. The true position of the emitter is marked by a green dot. The position estimate of the S⁴TDOA method is shown by a yellow x, the respective DS⁴TDOA estimate by a red circle. The achieved localization accuracy is given in Table I.

TABLE I
Localization accuracy in [m] of field experiments data.

RSS	S⁴TDOA	DS⁴TDOA	RSS	S⁴TDOA	DS⁴TDOA
−80	4049	385	−69	1003	129
−79	889	257	−68	2026	82
−78	681	449	−67	1542	190
−77	842	223	−66	186	166
−76	1203	50	−65	161	179
−75	1424	451	−64	170	268
−74	1272	89	−63	312	141
−73	1374	145	−62	458	404
−72	1623	116	−61	258	66
−71	1546	112	−60	199	119
−70	901	332			

As can be seen in Fig. 10, the minimum of the cost function of the S⁴TDOA for a received signal strength threshold level of $P_t = -74$ dBm is not located at the true emitter position due to the choice of one or more faulty TOA values (maximum peaks of the CCF). This results in a larger localization error. Here, the advantage of the DS⁴TDOA approach can be seen. Fig. 11 depicts the cost function of the DS⁴TDOA method for the same scenario. As can be observed, the minimum of the cost function is located near the true emitter position and the localization result is more accurate. For this scenario with a received signal strength threshold of $P_t = -74$ dBm, the 3-D localization error of the S⁴TDOA is 1272 m. Using the DS⁴TDOA localization algorithm, the position estimation error is 89 m.

The cost function of the S⁴TDOA and a received signal strength threshold of $P_t = -60$ dBm is shown in Fig. 12. Less measurements are used to localize the emitter, but due to the higher signal level, the choice of the peak of the CCF as TOA value tends towards the correct peak. With more accurate TDOA estimation, the localization result becomes more accurate. The cost function using the direct localization method (Fig. 13) is

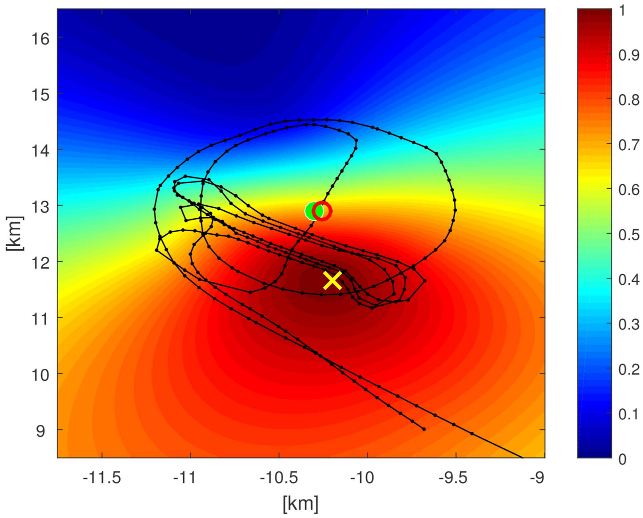

Fig. 10. Normalized cost function for S^{4}TDOA (signal threshold −74 dBm).

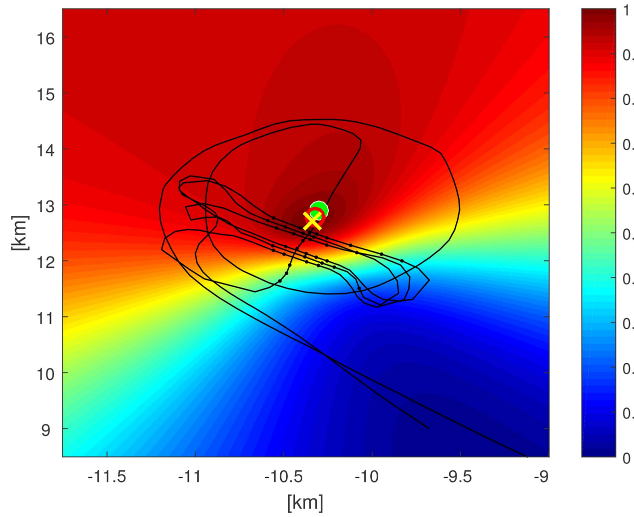

Fig. 12. Normalized cost function for S^{4}TDOA (signal threshold −60 dBm).

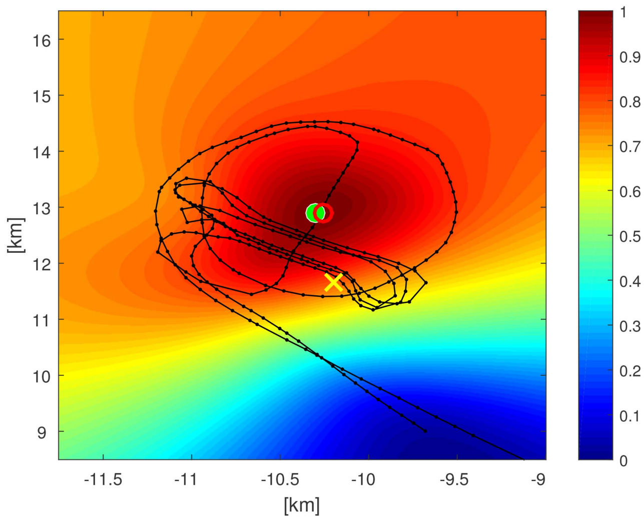

Fig. 11. Normalized cost function for DS^{4}TDOA (signal threshold −74 dBm).

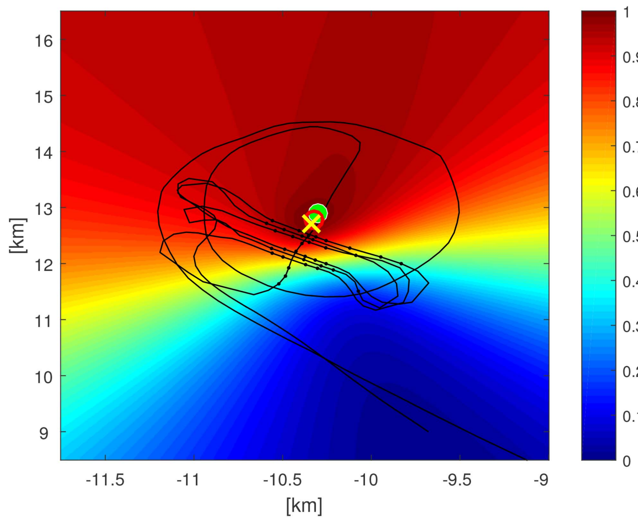

Fig. 13. Normalized cost function for DS^{4}TDOA (signal threshold −60 dBm).

very similar to the afore mentioned, also the localization results are nearly the same.

The localization accuracy for the S^{4}TDOA improves from 1272 m ($P_t = -74$ dBm) to 199 m ($P_t = -60$ dBm). For the DS^{4}TDOA location estimation method, a slight degradation of accuracy from 89 m ($P_t = -74$ dBm) to 119 m ($P_t = -60$ dBm) is noticed.

Fig. 14 shows the comparison of the localization errors of both methods over different signal strength levels. It can be observed, that the DS^{4}TDOA method is more robust to smaller received signal strength and outperforms the S^{4}TDOA-based method. As the TOA estimation using the signal structure information relies on the amplitude of the signal, with lower SNR, the TOA estimation becomes more and more noisy up until peaks that do not correspond to the signal are chosen as TOA. Since the DS^{4}TDOA method does not require choosing one peak of the CCF, the localization results remain more stable for lower signal level values.

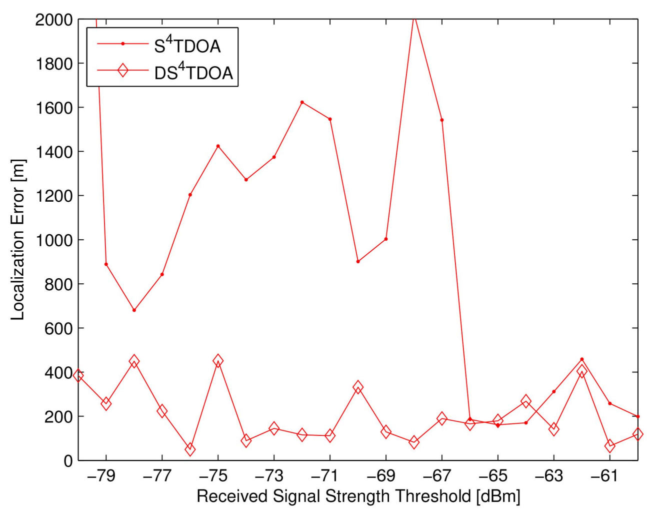

Fig. 14. Localization accuracy for different received signal strength thresholds of field experiment data.

C. Discussion

A large amount of localization error of a real world TDOA system can be caused by time and position inaccuracies of the sensors. In our experiments, we used GPS to determine the observers position during the flight. Especially the elevation estimation of a GPS receiver is known to be imprecise. Although we employed GPS disciplined oscillators, the time synchronization error might be the largest cause of localization error. In the case of stationary observers, a synchronization to UTC in the range of 25 ns is achievable. For in-flight use, the accuracy of the local clock can degrade up to 200 ns. Even though an exact time stamp is not necessary for the (D)S^4TDOA$^{(*)}$ methods, the employed experimental system allows only processing of one seconds of signal each five seconds. If continuous streaming of data is possible, a stable oscillator without exact time information is sufficient (the accuracy issue remains the same). Another real world error lies in the clock accuracy of the emitter which needs to be stable enough for all (D)S^4TDOA$^{(*)}$ methods to be applicable.

VIII. CONCLUSION

We evaluated four (direct) localization approaches for the use with a single moving sensor. The methods are based on the S^4TDOA found in [13]. The direct localization solution DS^4TDOA firstly introduced in [14] is derived in Section IV-B. The performance in means of emitter localization accuracy of S^4TDOA and DS^4TDOA are evaluated in simulations (Section VI). Field experiments dealing with the localization of GSM base stations using a single airborne sensor are presented in Section VII. Additionally, two methods (D)S^4TDOA* that do not require the explicit representation of the signal structure are introduced in Section IV-D. All four approaches are evaluated in Monte-Carlo simulations and compared to the CRLB (Section V).

All presented methods allow emitter localization with a light weight and small sensor node. Only one reception channel combined with an omni-directional antenna is needed. The requirements on the communication channel bandwidth between sensor and situation display system are small. Even if the position estimate is not determined at the sensor node but is calculated at a control station on ground, for (D)S^4TDOA only CCF and corresponding time and position information need to be transmitted. Classic TDOA approaches require the transmission of raw signal data to a reference sensor or control station, thus having higher demands on the communication channel.

If processing power and storage capacity is not a limiting factor, direct localization using DS^4TDOA* is shown in simulations to give the best localization results.

The feasibility of determining the position of an emitter using (D)S^4TDOA$^{(*)}$ is shown. The proposed DS^4TDOA$^{(*)}$ direct localization is more robust to smaller SNR and outperforms the S^4TDOA$^{(*)}$ localization in both simulations and field experiments.

REFERENCES

[1] A. Amar and A. J. Weiss
Direct geolocation of stationary wideband radio signal based on time delays and doppler shifts,
in *Proc. 15th Workshop on Statistical Signal Processing*, Cardiff, Wales, Sep. 2009, pp. 101–104.

[2] K. Becker
An efficient method of passive emitter location,
IEEE Trans. Aerosp. Electron. Syst., vol. 28, pp. 1091–1104, Oct. 1992.

[3] ———
Target Motion Analysis (TMA),
in *Advanced Signal Processing Handbook*, S. Stergioulos, Ed. New York, NY: CRC Press, 2001, ch. 9, pp. 284–301.

[4] M. L. Fowler
Analysis of single-platform passive emitter location with terrain data,
IEEE Trans. Aerosp. Electron. Syst., vol. 37, pp. 495–507, Apr. 2001.

[5] M. L. Fowler and X. Hu
Signal models for TDOA/FDOA estimation,
IEEE Trans. Aerosp. Electron. Syst., vol. 44, pp. 1543–1550, Oct. 2008.

[6] R. Kaune, D. Musicki, and W. Koch
On passive emitter tracking in sensor networks,
in *Sensor Fusion and its Applications*, C. Thomas, Ed. InTech, 2010, ch. 13, pp. 293–318.

[7] Z. Madadi, F. Quitin, and W. P. Tay
Periodic rf transmitter geolocation using a mobile receiver,
in *Proc. IEEE International Conference on Acoustics, Speech and Signal Processing (ICASSP)*, South Brisbane, QLD, Australia, Apr. 2015, pp. 2584–2588.

[8] M. Oispuu
Direct state determination of multiple sources with intermittent emission,
in *Proc. 17th European Signal Processing Conference*, Glasgow, Scotland, Aug. 2009, pp. 1948–1952.

[9] M. Oispuu and U. Nickel
Direct detection and position determination of multiple sources with intermittent emission,
Signal Processing, vol. 90, pp. 3056–3064, Dec. 2010.

[10] M. Pourhomayoun and M. L. Fowler
Distributed computation for direct position determination emitter location,
IEEE Trans. Aerosp. Electron. Syst., vol. 50, pp. 2878–2889, Oct. 2014.

[11] F. Quitin, Z. Madadi, and W. P. Tay
Rf transmitter geolocation based on signal periodicity: Concept and implementation,
in *Proc. IEEE International Conference on Communications (ICC)*, London, England, Jun. 2015, pp. 4593–4598.

[12] S. V. Schell and W. A. Gardner
High-resolution direction finding,
in *Handbook of Statistics, Signal Processing and its Applications*, N. K. Bose and C. R. Rao, Eds. Elsevier, 1993, vol. 10, ch. 18, pp. 755–817.

[13] C. Steffes
Novel TDoA-based single sensor localization approach using signal structure information,
in *Proc. 12th Workshop on Positioning, Navigation and Communication (WPNC)*, Dresden, Germany, Mar. 2015.

[14] C. Steffes and M. Oispuu
Direct Single Sensor TDOA Localization Using Signal Structure Information,
in *18th International Conference On Information Fusion (FUSION)*, Washington, D.C., USA, July 2015.

[15] S. Stein
Algorithms for ambiguity function processing,
IEEE Trans. Acoust., Speech, Signal Processing, vol. 29, pp. 588–599, Jun. 1981.

[16] D. J. Torrieri
Statistical theory of passive location system,
IEEE Trans. Aerosp. Electron. Syst., vol. 20, pp. 183–198, Mar. 1984.

[17] E. Tzoreff, B. Z. Bobrovsky, and A. J. Weiss
Single receiver emitter geolocation based on signal periodicity with oscillator instability,
IEEE Trans. Signal Processing, vol. 62, pp. 1377–1385, Feb. 2014.

[18] A. J. Weiss
Direct position determination of narrowband radio frequency transmitters,
IEEE Signal Processing Lett., vol. 11, pp. 513–516, May 2004.

[19] A. J. Weiss and A. Amar
Direct position determination of multiple radio transmitters,
in *Advances in Direction-of-Arrival Estimation*, S. Chandran, Ed. Norwood, MA: Artech House, 2006, ch. 11, pp. 213–239.

[20] A. Yeredor and E. Angel
Joint tdoa and fdoa estimation: A conditional bound and its use for optimally weighted localization,
IEEE Trans. Signal Processing, vol. 59, pp. 1612–1623, Apr. 2011.

Christian Steffes received his Diploma in Computer Science at University of Bonn, Germany. Since 2010 he works at Fraunhofer Institute for Communication, Information Processing and Ergonomics FKIE, Wachtberg, Germany, in the department Sensor Data and Information Fusion. His research is focused on passive emitter localization.

Marc Oispuu received the diploma degree in electrical engineering from the RWTH Aachen, Germany, in 2005. Currently he is a research assistant with the Department of Sensor Data and Information Fusion at Fraunhofer Institute for Communication, Information Processing and Ergonomics FKIE, Wachtberg, Germany. Additionally he achieved his Ph.D. degree at the Center for Sensor Systems, University of Siegen, in 2013. His research interests focus on passive emitter localization and advanced array signal processing.